Model-based segmentation of aortic ultrasound images

Hrvoje Kalinić and Sven Lončarić
Universiy of Zagreb, Faculty of
Electrical Engineering and Computing,
Department of Electronic Systems
and Information Processing,
10000 Zagreb, Croatia
e-mail: hrvoje.kalinic@fer.hr

Maja Čikeš and Davor Miličić
Universiy of Zagreb,
School of Medicine,
Department for Cardiovascular Diseases,
University Hospital Centre Zagreb,
10000 Zagreb, Croatia

Bart Bijnens
Catalan Institution for Research
and Advanced Studies,
and Universitat Pompeu Fabra
E08003 Barcelona, Spain

***Abstract*—Morphological features of the aortic outflow ultrasound images are used in clinical practice for diagnosis of cardiovascular diseases. While feature extraction can be done manually, it is very time consuming. Segmentation is an important step in image interpretation, analysis, and quantification of the objects within a scene. In this work, we propose a novel method for the automatic segmentation of aortic outflow profiles based on a segmentation technique that incorporates a prior knowledge about the object shape in the form of the shape boundary model. The proposed model-based method utilizes a series of image analysis steps including image registration and a modification of the RANSAC algorithm to deal with noise and other artifacts in the image acquisition process. The experimental validation is done on a set of 67 patients and is compared to manual segmentation by an expert cardiologist. The proposed method has shown high correlation with results obtained by the expert cardiologist.**

I. Introduction

The Continuous Wave Doppler signal represents the time-change of velocities along a scan line in a 2-D ultrasound imaging plane. The signal generated by the blood outflow from the heart into aorta, acquired by Continuous Wave Doppler, is known as the aortic outflow profile (see Figure 1). In this study, we are interested in detecting the shape of the aortic outflow profile, since morphological characteristics of the aortic outflow profile can be used in clinical practice for the assesment of cardiovascular diseases. To be able to find a correlation between the aortic outflow profile morphology and the myocardial function, segmentation of the profile is necessary. Following the segmentation, the quantification of morphological characteristics is possible. While the segmentation can be done manually, it is usually time consuming. In this manuscript, we propose a novel method for automatic segmentation of aortic outflow profiles based on a segmentation technique that incorporates a prior knowledge about the object shape in the form of shape boundary model. The proposed method utilizes (1) region-based thresholding to find the rough shape boundary, (2) boundary modeling and model fitting, and (3) a modified version of the RANSAC algorithm to deal with possible inaccuracies of the previous steps.

Tschirren et al. [1] and Bermejo et al. [2] have worked on blood velocity profiles. Tschirren et al. analyses brachial artery blood flow and therefore does not deal with the problems such as valve click (described later), while Bermejo et al. utilize a manual segmentation of the blood flow in their study. Our previous work [3], [4], described a solution to the problem of aortic outflow segmentation using an anatomical atlas. Atlas construction and image registration are computationally intensive operations which include a complex spatial transform and optimization procedure. Therefore, in this paper, we investigate a different approach which is inherently less computationally intensive. The approach is based on boundary modeling in the form of a (truncated) harmonic decomposition, similar to the Fourier or Sine transform [5], [6], [7]. Due to various artifacts and excessive noise, the model fitting using linear regression [8] is heavily affected by the large number of outliers. To deal with this, a random sample consensus [9] is used to select the best fit of the model on the given data. In the rest of the paper, we first describe the problems which make ultrasound image segmentation a challenging problem, and then we proceed with the methodology and problem solution explanation.

The methodology proposed herein is evaluated on aortic outflow images from of 13 healthy volunteers and 54 patients with aortic stenosis. Images were acquired with a clinical echocardiographic scanner (Vivid 7, GE Healthcare) using an apical 5-chamber view and Continuous Wave Doppler mode. Images were digitally stored in 'raw' Dicom format, containing the spectral Doppler information in proprietary tags. Using an Echopac workstation (GE Healthcare), the 'raw' Dicom images were converted into Hierarchical Data Format (HDF). From the HDF image the aortic outflow profile was extracted. The aortic outflow profile image reflects the time-change of aortic velocities, with the x-axis representing time and y-axis the velocities.

II. Problem specification

Segmentation of ultrasound images is difficult due to problems such as image noise, various acquisition artifacts, and poor contrast. Some of these problems are depicted in Figure 1. The object within the white ellipsoid in the Figure 1(a) is the object that needs to be segmented. This object represents the motion along the scanning line when the heart valves are open

i.e. when the blood flows form the heart into the aorta. Notice that the region of interest is usually the largest bright region within image, however, this is not always the case, as we can see in the Figure 1(d).

The low velocity rejection region depends on the machine settings (clutter filter), and can significantly vary in size (see Figure 1(b)) depending on the user's settings. This velocity rejection region may present a problem for a region based approach to image segmentation since it may arbitrarily vary around zero and occlude the low velocities of the object of interest. To quantify the time-change of the velocities, or simply to discard the negative velocities, the line that represents the zero velocity needs to be identified. This will be the object's lower boundary. Similarly, the upper object border is bound by the instantaneous maximal velocity of the blood flow. However, the artifacts, similar to the ones indicated by the ellipsoids in the Figure 1(c), introduce additional difficulties in detecting the object upper boundary. To ease this problem, we first detect the velocity line above which there is no significant information, somewhat alike the zero velocity line. In many cases, this approach will discard artifacts such as aliasing, but the valve clicks will surely remain. The valve clicks represent a portion of the signal concatenated to the end or the beginning of the region of interest which arise at valve opening and closing. This obviously distorts the information about blood outflow velocities, since in many cases the maximal velocity recorded by Doppler ultrasound does not represent the maximal blood outflow velocity but rather the maximal valve velocity. Therefore we should also discard the valve clicks from the object.

As noticed earlier, the objects within the region of interest vary in brightness and contrast, sometimes even within the same image. A constant threshold level would obviously lead to an object with many holes (at least in some cases) and a noisy border.

III. Method

The outline of the proposed method is shown below:

1) determine zero-velocity line (lower signal boundary)
2) determine maximal-velocity line (upper signal boundary)
3) apply median filter for image noise reduction
4) extract individual heart beats
5) register individual heart beat images by correlation
6) average registered heart beat images
7) select threshold value
8) perform image thresholding to obtain initial segmentation result
9) fit velocity profile model using the RANSAC algorithm to improve segmentation result

A. Lower and upper signal boundary

To detect the lower and upper signal boundary, the image is projected onto the y-axis. Afterwards, the image projection is smoothed, divided by 2, and plotted together with the image projection, as shown in Figure 2. Now, the low velocity region is easily recognized as the part of the signal for which the smoothed projection is higher than the original signal. The zero-velocity line is defined as the medial part of this region. The maximal-velocity line is detected as the rise of the smoothed projection by 10% from the end of the signal.

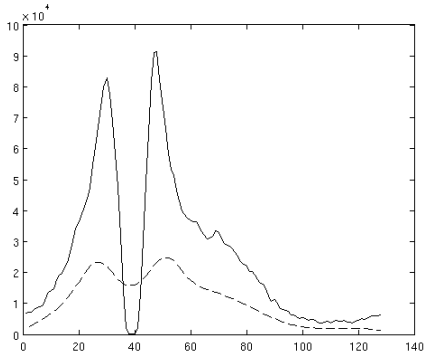

Fig. 2. The projection of the image onto the y-axis (solid line) and smoothed signal divided by 2 (dotted line). x-axis is in pixels, y-axis shows the sum of intensities.

The smoothing of the projection of the image onto the y-axis is done using the convolution between the original signal and the Gaussian filter of size N=10.

B. Noise reduction

Since we primarily expect speckle noise in the images, two median filters were introduced. This is done just after the zero-velocity line detection, to avoid the low velocity region blurring in cases when this region is rather thin. The mask of the first median filter is 3-by-3, while the second mask dependents on the size of the original image. In the case the image size is M-by-N, the mask will have the size (M-by-N)/100. The result is rounded to integer.

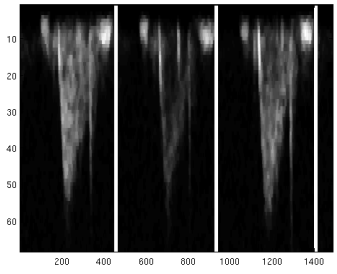

Fig. 3. An example of the detected period. Both axis are in pixels.

C. Heart beat extraction and averaging

For additional noise reduction, the fact that cardiac signals are periodic is used. First, the period of the signal is detected. This is done by a multi-resolution approach. At a lower resolution, the correlation is done between the first part of

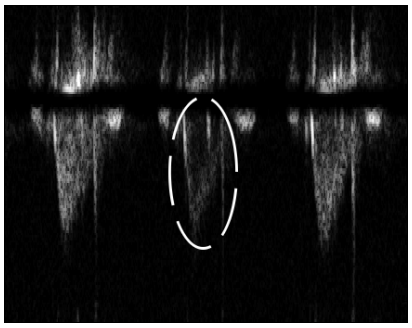

(a) Dashed ellipsoid indicates problem with the poor contrast

(b) Dashed ellipsoid indicates the low velocity region

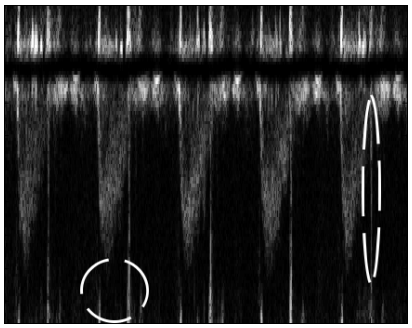

(c) Dashed ellipsoid indicates artifacts (referred by cardiologist as aliasing and valve clicks)

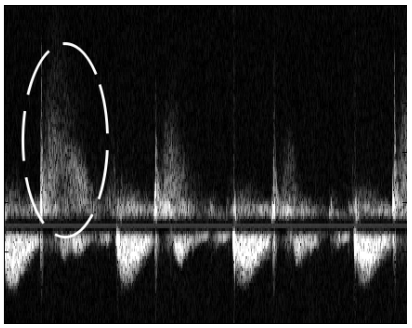

(d) Dashed ellipsoid indicates largest bright region

Fig. 1. The figure depicts the issues with the region-based approach of the aortic profile detection and segmentation, such as poor contrast (a), large low velocity region (b), various artifacts (c), and other bright region apart from region of interest (d).

the image, and the next part of the same size. This is repeated by iteratively adding pixel columns to the images. The period is detected at the point where the maximal image correlation is achieved. The same procedure is repeated at a higher resolution, to detect the period more accurately. The example of the detected period is depicted in the Figure 3.

After the cardiac period is detected, the image of each heart beat is extracted and the average heart beat image is calculated.

D. Threshold selection

The threshold is selected as the average intensity (denoted by A) from the average beat image. Image thresholding is performed using the selected threshold value to obtain a rough initial segmentation result. Figure 4 shows the result for a representative image.

E. Model fitting

After thresholding the object boundary is visible. The border represents the envelope of the signal, but not the maximal velocity of the blood outflow since some of the signals still contains the valve clicks. However, working with the envelope of the signal, rather than the whole image, we may significantly improve the execution time. Furthermore, this is not the desired signal, since the interval of interest is much smaller than the average beat. The beginning and the end of the interval of interest is depicted by two white circles in Figure 4 (denoted with x_0 and x_{end}). To detect the region of interest within the average beat, the algorithm searches for the part

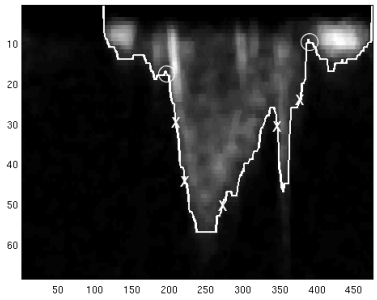

Fig. 4. Point selection for the approximation algorithm.

of the envelope higher than the average, and focuses to the part of the signal that has the longest duration. This region is enlarged until the envelope stops falling. This is used just as an approximation of the beginning and the end of the signal. The real beginning and the and of the signal are randomly selected, within the implementation of the RANSAC algorithm, from an uniform distribution around that value. The interval for the uniform distribution was selected as 10% of the interval of interest for the signal beginning and 30% for the signal end.

The envelope of the outflow profile within the interval of interest can be modeled using a set of sine functions. The idea behind this approach is that the valve clicks, that may exist within this interval and occlude the information about the blood outflow velocities, have higher frequency than

the frequency allowed by the model proposed below. In this way the valve clicks will be treated as the outliers from the proposed model which the RANSAC algorithm has to deal with. If we pick just one point from the envelope within the region of interest (let's denote it (x, y)), an approximation of a signal can be written as:

$$y = \sum_{i}^{M} a_i \cdot sin(\frac{i\pi(x - x_0)}{l}) \tag{1}$$

where l is the length of the signal, i.e. $l = x_{end} - x_0$, and M is the number of sine functions used for signal approximation. We selected $M = 4$. From the region of interest N points are selected and used to model the envelope (denoted as white "X" in Figure 4). Notice that with $N = 5$ points selected, the equation system is overdetermined and can be written in matrix form as:

$$\begin{bmatrix} sin(\frac{\pi(x_1-x_0)}{l}) & ... & sin(\frac{M\pi(x_1-x_0)}{l}) \\ ... & . & ... \\ sin(\frac{\pi(x_N-x_0)}{l}) & ... & sin(\frac{M\pi(x_N-x_0)}{l}) \end{bmatrix} \cdot \begin{bmatrix} a_1 \\ . \\ . \\ a_M \end{bmatrix} = \begin{bmatrix} y_1 \\ . \\ . \\ y_N \end{bmatrix} \tag{2}$$

We used the notation $\mathbf{x} = [x_1..x_N]^T$ and $\mathbf{y} = [y_1..y_N]^T$ for the coordinates of the samples from the envelope (Figure 4), and $\mathbf{a} = [a_1..a_M]^T$ to denote the vector of the amplitudes of each sine component used to model the envelope. If Equation 2 is written in the more compact form:

$$S \cdot \mathbf{a} = \mathbf{y} \tag{3}$$

it is easy to notice that the solution of Equation 3 can be given as the mean squared error approximation. So the vector of the amplitudes of the sine components (vector $\mathbf{a}$) used to model the envelope is calculated as:

$$\mathbf{a} = S^{+} \cdot \mathbf{y} \tag{4}$$

where S^{+} stands for a Moore-Penrose pseudoinverse of a matrix S [10], [11].

While in the best case scenario, the approximation of the signal removes the noise from the signal, it may still happen that, due to the selection of the points, the approximation may not be so good. The approximation depends on just M selected points from the signal and some of the selected points may be selected from the part of the envelope belonging to the valve click. This part of the envelope bears no significant information of the blood outflow, but may significantly change the proposed approximation. Therefore, these points should be considered as outliers. To deal with outliers a modified version of the RANSAC algorithm was implemented. Apart from the randomly selected points from the region of interest and search for the best consensus of the signal approximation, the random selection of the beginning and ending point was also implemented. This was done since it was noticed that the quality of the approximation is heavily dependent on these two points, which are impossible to determine exactly without use of expert knowledge.

IV. Evaluation and results

To evaluate the proposed method 67 images of outflow velocity profiles are used. 13 out of 67 images belong to healthy volunteers, while the rest (54 images) belonged to patients with severe aortic stenosis. The images range in resolution from 96-by-1486 to 128-by-2890, with 8-bit encoding of the intensity levels. The proposed segmentation is compared to manual segmentation done by an expert cardiologist. The results are evaluated in the following way: a) by measuring the segmentation error defined as in Equation 5 and b) by measuring the correlation between delineated border of automated and manual segmentation.

The segmentation error is defined by:

$$E = \frac{A_1 - A_2}{A} \tag{5}$$

where A_1 is the area of the manually segmented region, A_2 is the area of the region segmented using the proposed method for aortic outflow segmentation, and the area A is defined as $A = A_1 \cup A_2$. For qualitative evaluation, an example of an aortic outflow profile segmentation is presented in Figure 5. In the left figure, the manual segmentation is depicted with a dashed line, and on the right figure the dashed line represents the result of the simple thresholding technique described earlier (see Section III-D). In both figures, the solid line shows the result of the proposed method.

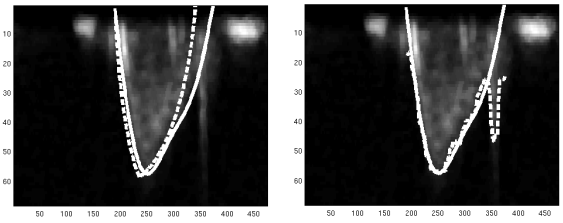

Fig. 5. The comparison of the manual and the proposed segmentation (left) and the comparison of the proposed segmentation and simple thresholding (right). All axis are in pixels. See text for details.

Notice how in Figure 5 manual and automated segmentation results correlate well, while the method manages to deal with noise and outliers. This is generally the case, since the average correlation is 89.87%. An average error (calculated as in Equation 5) is 20.25%. To quantify how well the segmentation method tracks the perceptual border of an object, we measured the average intensity standard deviation along the delineated border. The average intensity standard deviation along the delineated border is 27.95 for the proposed segmentation, and 15.52 for the manual segmentation. This equals to 10.96%, or 6.08% respectively, since each image has the maximum value of 255.

V. Conclusion and Future Work

In this paper, a model-based approach for Doppler velocity profile segmentation has been proposed. It incorporates a preprocessing step, envelope detection and model fitting which

deals with outliers using a version of the RANSAC algorithm. The proposed method was evaluated on the 67 outflow velocity profiles from a combined set of healthy volunteers and patients with aortic stenosis. The results showed a high correlation (89.87%) with manual segmentation and an average error of 20.25%. We believe that the method shows promising results since the results presented here may be additionally improved if the heart beat period is more accurately detected. This can be achieved either by manual indication of the period, either by working directly with DICOM files which contain also the ECG signal.

REFERENCES

[1] J. Tschirren, R. M. Lauer, and M. Sonka, "Automated analysis of doppler ultrasound velocity flow diagrams," *IEEE Trans. Med. Imaging*, vol. 20, no. 12, pp. 1422–1425, 2001.

[2] J. Bermejo, J. C. Antoranz, M. A. García-Fernández, M. M. Moreno, and J. L. Delcán, "Flow dynamics of stenotic aortic valves assessed by signal processing of doppler spectrograms," *Am J Cardiol*, pp. 611–617, 2000.

[3] H. Kalinic, S. Loncaric, M. Cikes, D. Milicic, I. Cikes, G. Sutherland, and B. Bijnens, "A method for registration and model-based segmentation of doppler ultrasound images," *Medical Imaging 2009: Image Processing*, vol. 7259, no. 1, p. 72590, 2009.

[4] H. Kalinić, S. Lončarić, M. Čikeš, D. Miličić, and B. Bijnens, "Image registration and atlas-based segmentation of cardiac outflow velocity profiles," *Computer Methods Programs Biomedicine*, 2010. [Online]. Available: http://dx.doi.org/10.1016/j.cmpb.2010.11.001

[5] A. D. Poularikas, Ed., *The Transforms and Applications Handbook*, 2nd ed., ser. The Electrical Engineering Handbook Series. CRC Press, 2000.

[6] G. Chirikjian and A. Kyatkin, *Engineering Applications of Noncommutative Harmonic Analysis*. CRC Press, 2001.

[7] J. L. Semmlow, Ed., *Biosignal and Biomedical Image Processing MATLAB based Applications*. Marcel Dekker, Inc., 2004.

[8] S. Chatterjee and A. S. Hadi, "Influential observations, high leverage points, and outliers in linear regression," *Statistical Science*, vol. 1, no. 3, pp. 379–393, 1986.

[9] M. A. Fischler and R. C. Bolles, "Random sample consensus: a paradigm for model fitting with applications to image analysis and automated cartography," *Commun. ACM*, vol. 24, no. 6, pp. 381–395, June 1981.

[10] E. H. Moore, "On the reciprocal of the general algebraic matrix," *Bulletin of the American Mathematical Society*, vol. 26, pp. 394–395, 1920.

[11] R. Penrose, "A generalized inverse for matrices," *Proceedings of the Cambridge Philosophical Society*, vol. 51, pp. 406–413, 1955.